

## Design of Ferrocene Organothiol Monolayer as Intermediate Phase for Miniaturized Electrochemical Sensors with Gold Contact<sup>\*</sup>

by S. Sęk<sup>1</sup>, R. Bilewicz<sup>1\*\*</sup>, E. Grygółowicz-Pawlak<sup>2</sup>, I. Grudzień<sup>2</sup>,  
Z. Brzózka<sup>2</sup> and E. Malinowska<sup>2\*\*</sup>

<sup>1</sup>*Department of Chemistry, University of Warsaw, Pasteura 1, 02-093 Warsaw, Poland*

<sup>2</sup>*Department of Chemistry, Warsaw University of Technology, 00-664 Warsaw, Poland*

*(Received March 16th, 2004; revised manuscript April 26th, 2004)*

New design of back side contact (BSC) chips for miniaturized electrochemical sensors with Au contact modified by monolayers of purposely synthesized organothiol molecules is described. Voltammetric studies of the monolayers indicate reversible behavior of the compounds and efficient coverage of the gold electrode. Properties of 5 compounds are compared. The electroactive benzenethiol based self-assembled monolayer is selected as a convenient intermediate layer in solid contact potentiometric sensors since it forms a hydrophobic barrier between the electrode and the solution and at the same time provides efficient electronic wiring to the electrode. Stable electrode performance is obtained and the potentiometric response remains as fast as using bare gold contact which should be favorable for the application of the described intermediate layers in ion-selective electrodes.

**Key words:** intermediate layer for solid contact potentiometric sensors, self-assembled monolayers, redox-active organothiols

Ion selective electrodes with ion-selective polymeric membrane coated directly on a metallic conductor belong to the group of solid-contact sensors. Complete elimination of the internal electrolyte solution was found to affect the electrochemical stability of these sensors, which was explained as due to the not well thermodynamically defined interface between the polymeric membrane and solid conductor [1–3]. To overcome this problem, several approaches were proposed, *e.g.* the incorporation lipophilic silver-ligand complexes within polymeric films [4], polymer layer that is redox-active [3] or conducting polymers [5–11]. The improvement of the stability of such sensors was achieved by establishing reversible electron transfer at the membrane/solid contact interface. Recently, improved potential stability and at the same time removal of interferences of redox impurities and oxygen were reported for sensors with redox-active self-assembled monolayers (SAMs) as the intermediate phase [12,13]. SAMs of fullerene and tetrathiafulvalene derivatives served as intermediate layer between an ion-selective membrane and a solid Au contact due to formation of well defined electron acceptor – electron donor couple.

---

<sup>\*</sup> Dedicated to Prof. Dr. Z. Galus on the occasion of his 70th birthday.

<sup>\*\*</sup> Authors for correspondence.

In this work, we propose a different strategy for separating the metallic conductor from the solution phase. Ferrocene terminated organothiols containing amide or benzene moieties are probed as potential components of the intermediate layers for solid-state sensors. In our previous papers we have shown that systematic studies of well-defined donor-bridge-acceptor systems can simplify the analysis of electron transfer pathways [14–17]. We have demonstrated that monolayers of thiolated compounds self-assembled on metal electrodes can serve as useful model systems for the studies of kinetics of mediated electron transfer. Electron or hole transfer between a given donor (D) and acceptor (A) can be modulated by changing the distance separating them or by chemical modification of the linking unit. In the present work, well organized monolayer assemblies of various molecules with amide and benzene moieties are studied using the voltammetric method in order to establish the efficiency and reproducibility of the electrode coverage, and the reversibility of the ferrocene electrode processes. The monolayers are used as molecular junctions providing electronic connection with the electrode but at the same time serving as efficient hydrophobic spacer eliminating direct access of the solution species to the gold surface.

## EXPERIMENTAL

**Synthesis of compounds.** Long chain disulfides (1)  $(S-(CH_2)_2-NHCO-(CH_2)_{11}-NHCO-Fc)_2$  and (2)  $(S-(CH_2)_2-NHCO-(CH_2)_{10}-NHCO-Fc)_2$  were synthesized using previously described procedures [14–16]. Disulfides (3)  $(S-(CH_2)_2-NHCO-Fc)_2$  and (4)  $(S-C_6H_4-NHCO-Fc)_2$  were obtained by coupling reaction between the ferrocenemonocarboxylic acid and 4-aminophenyl disulfide or cystamine, respectively. The coupling reaction was carried out in DMF in the presence of coupling reagent *O*-(benzotriazol-1-yl)-*N,N,N',N'*-tetramethyluronium hexafluorophosphate. All synthesized components were characterized by NMR: (1)  $(S-(CH_2)_2-NHCO-(CH_2)_{11}-NHCO-Fc)_2$  –  $^1H$  NMR ( $CDCl_3$ ),  $\delta$  (ppm): 1.20–1.60 (broad overlapping resonance, 36H); 2.24 (t,  $J = 7$  Hz, 4H); 2.88 (t,  $J = 7$  Hz, 4H); 3.60 (broad, 8H); 4.24 (s, 10H); 4.36 (s, 4H); 4.69 (s, 4H); 6.03 (broad s, 2H); 6.72 (broad s, 2H). (2)  $(S-(CH_2)_2-NHCO-(CH_2)_{10}-NHCO-Fc)_2$  –  $^1H$  NMR ( $CDCl_3$ ),  $\delta$  (ppm): 1.20–1.70 (broad overlapping resonance, 32H); 2.22 (t,  $J = 7$  Hz, 4H); 2.88 (t,  $J = 7$  Hz, 4H); 3.56 (broad, 8H); 4.24 (s, 10H); 4.38 (s, 4H); 4.74 (s, 4H); 6.01 (broad s, 2H); 6.76 (broad s, 2H). (3)  $(S-(CH_2)_2-NHCO-Fc)_2$  –  $^1H$  NMR ( $CDCl_3$ ),  $\delta$  (ppm): 2.99 (broad, 4H); 3.75 (broad, 4H); 4.26 (s, 10H); 4.39 (s, 4H); 4.82 (s, 4H); 6.62 (broad s, 2H). (4)  $(S-C_6H_4-NHCO-Fc)_2$  –  $^1H$  NMR ( $CDCl_3$ ),  $\delta$  (ppm): 4.46 (s, 10H); 4.70 (s, 4H); 5.10 (s, 4H); 7.52 (arom. m, 8H); 7.82 (broad s, 2H).

**Preparation of electrodes.** The back-side contact (BSC) silicon-based sensor chips were fabricated using standard IC technology. The subsequent procedures of the chips' preparation were the same as described previously [18,19], except for the last two electrochemical steps leading to silver/silver chloride layers (Fig. 1A). The evaporated gold layer (0.5  $\mu m$ ) was served as the sensing unit in the silicon structures described in the present paper (Fig. 1B).

To evaluate potentiometric properties of the obtained chips, they were placed in implants of a flow cell (for details of the cell construction see [20]). All potentiometric measurements were performed in the flow system at ambient temperature ( $21 \pm 1^\circ C$ ). The solution composition was changed by adding appropriate volumes of 0.1 M  $K_3Fe(CN)_6$  solution to the stirred solution of 0.01 M  $K_4Fe(CN)_6$ .

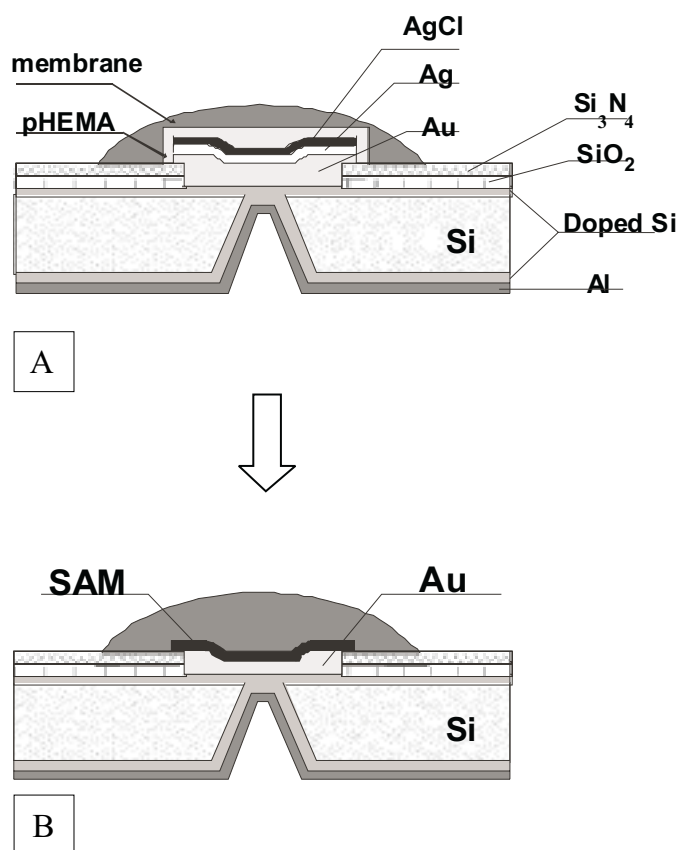


**Figure 1.** The schematic representation of changes in the structure of silicon-based BSC transducers. Chips with A) Ag/AgCl and B) Au sensing sites.

One component monolayers were prepared on the gold surfaces by the self-assembly method [21–23]. The gold substrates were immersed in 1 mM ethanolic solutions of disulfides (1)–(4) or alkanethiol (SAM 5) for a period of 24 h. After the self-assembly step, the modified substrates (Fig. 2) were rinsed with ethanol and water.

**Instrumentation and materials.** Cyclic voltammetry experiments were performed using three-electrode system, with gold substrate as working electrode, sodium saturated calomel electrode as the reference electrode and platinum foil as the counter electrode. Supporting electrolyte was 1M  $\text{HClO}_4$  and it was degassed before the measurements. A PAR 273 potentiostat, interfaced with personal computer was used to record cyclic voltammograms.

The EMF values were measured using a custom-made 10-channel electrode monitor, interfaced with personal computer [24]. The potentials of the examined sensors were measured *vs.* liquid junction Ag /AgCl/ 1 M KCl / 1 M  $\text{CH}_3\text{COOLi}$  reference electrode, placed centrally in the flow cell.

All chemicals were reagent grade. The nonelectroactive thiol,  $\text{CH}_3(\text{CH}_2)_5\text{SH}$ , was obtained from Aldrich. Water was triply distilled and passed through the MilliQ system. All experiments were done at room temperature.

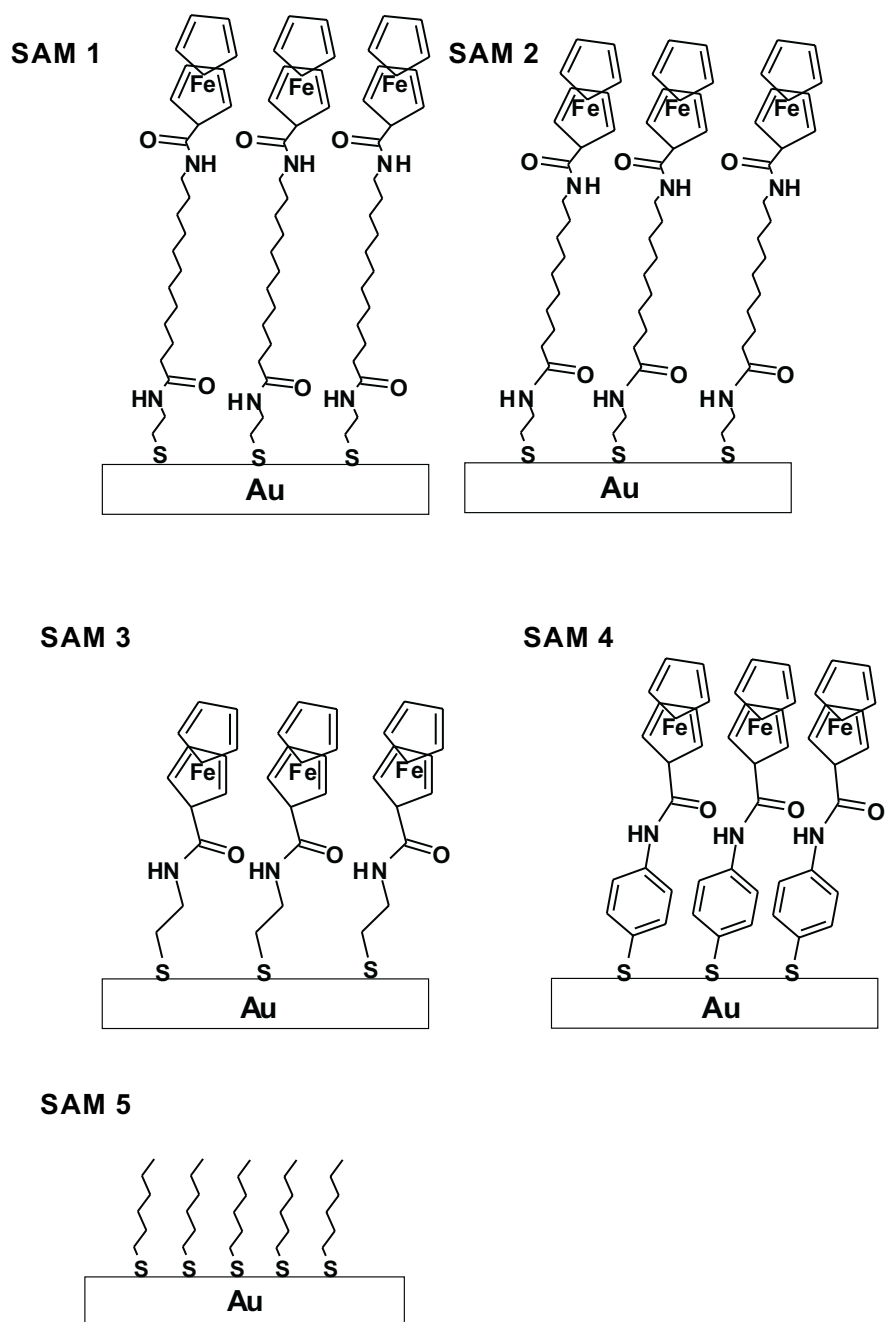


**Figure 2.** The structures of compounds assembled in monolayers on the metallic conductor.

## RESULTS AND DISCUSSION

**Potentiometric behavior of BSC chips with Au sensing contact.** Fig. 1A presents the miniaturized back side contact (BSC) planar ion-selective sensor based on silicon technology. Silicon structures in our previous paper [25] possessed Ag/AgCl layers serving as the internal electrode. The pHEMA layer containing appropriate electrolyte and introduced between polymeric membrane and Ag/AgCl layer of the chip was found to improve the EMF stability and reproducibility of the sensors [19,25]. In order to simplify the technology of sensor chips fabrication (two steps related to electrochemical silver and then silver chloride deposition can be eliminated), in the present paper, the gold film (Au) without the silver/silver chloride (Ag/AgCl) overlayers is employed (Fig. 1B).

The BSC chips with gold sensing contact play the role of an internal reference electrode of miniaturized ion-selective sensors. The miniaturized Au electrode, situated on the front side of the chip, should show the changes in EMF as a function of the ratio of oxidized to reduced form of redox species. In order to evaluate whether designed silicon structures can be used as transducers, the calibration curves for  $[\text{Fe}(\text{CN})_6^{3-}/\text{Fe}(\text{CN})_6^{4-}]$  and their response time have been examined (Fig. 3). The potentiometric response was examined over the  $\log[\text{Fe}(\text{CN})_6^{3-}/\text{Fe}(\text{CN})_6^{4-}] = -3.0 - 0.2$  range. The BSC sensors exhibited potentiometric characteristics almost identical to those obtained for classical Pt electrodes. The 10 randomly chosen sensors exhibited fast and reversible response to  $[\text{Fe}(\text{CN})_6^{3-}/\text{Fe}(\text{CN})_6^{4-}]$ . The response time ( $t_{95}$ ) was shorter than 12 s. Calibration curves of 10 sensors tested at the same time (Fig. 3) revealed that they can be fabricated in a very reproducible manner. Based on these results it can be concluded that BSC sensors with Au layer are useful for application in miniaturized potentiometric sensors. Chemical modification of such devices is done by the deposition of the ion-selective membranes on the sensing-site, in this case – miniaturized Au electrode of the chip. For the applications as ion-selective membrane sensors, a layer separating the conductor from the membrane should be designed as pointed out in the introduction. The replacement of pHEMA with a new type of intermediate layer meeting the requirements of well thermodynamically defined interface between the polymeric membrane and solid conductor (Au) assures stable performance of the sensors. For this purpose, a series of ferrocene terminated dithiols were prepared, and self-assembled on the Au contact (SAMs 1–5 – Fig. 2).

**Voltammetric behavior of gold electrodes modified with SAMs 1–4.** The redox behavior of the electroactive monolayer assemblies SAMs 1–4 was characterized by cyclic voltammetry (Fig. 4). Analysis was based on relevant parameters such as peak current, area, position and shape. Electrochemical data extracted from the voltammograms are collected in Table 1. Voltammograms shown in Figure 4 reveal characteristic symmetrical shape of curves characteristic for surface confined faradaic reactions. Moreover, the anodic peak current for each system was found to increase linearly with the scan rate, which is also indicative for adsorbed redox centers. All compounds under study show reversible electrochemical behavior, the peak separations ( $E_{p,a} - E_{p,c}$ ) at low scan rates (20–200 mV/s) were never larger than 30 mV.

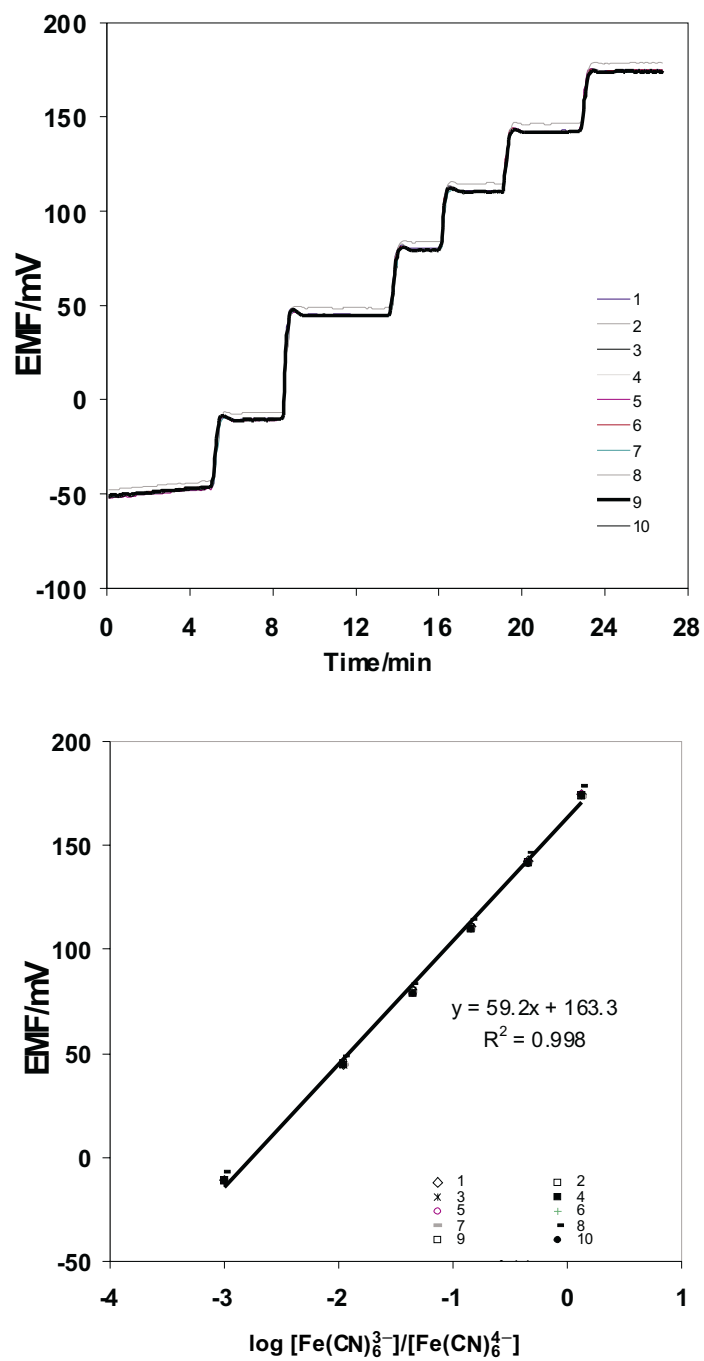


**Figure 3.** Potentiometric response to changes in  $\text{Fe(CN)}_6^{3-}$  and  $\text{Fe(CN)}_6^{4-}$  concentrations in sample solution. Randomly chosen 10 sensor chips with bare gold contact.

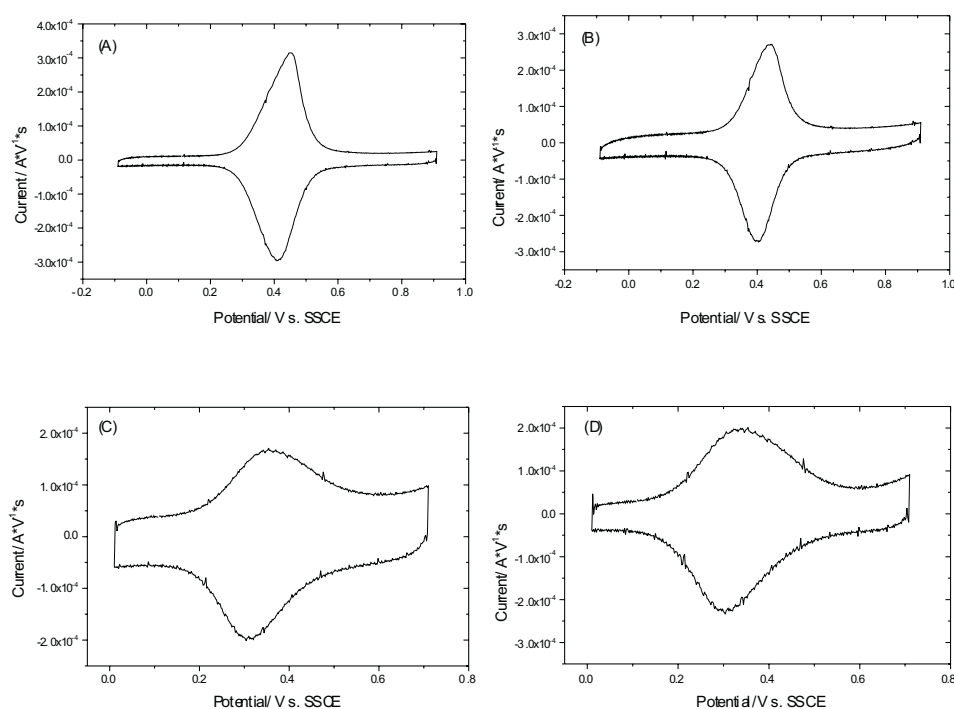


**Figure 4.** Cyclic voltammograms recorded with SAMs modified gold electrodes in 1M HClO<sub>4</sub> at scan rate 10 V/s. (A) SAM 1, (B) SAM 2, (C) SAM 3, (D) SAM 4.

**Table 1.** Characterization of electroactive monolayer assemblies SAMs 1–4.

Monolayer	Formal Potential [mV] vs. SSCE	Width of the Peak at Half Height [mV]	Surface Coverage [mol/cm <sup>2</sup> ] $\times 10^{10}$
SAM 1	+428 $\pm$ 4	126 $\pm$ 9	4.8 $\pm$ 0.4
SAM 2	+424 $\pm$ 10	110 $\pm$ 10	4.7 $\pm$ 0.5
SAM 3	+322 $\pm$ 7	160 $\pm$ 13	3.8 $\pm$ 0.7
SAM 4	+336 $\pm$ 6	172 $\pm$ 15	3.4 $\pm$ 0.5

Formal potentials calculated as  $(E_{p,a} + E_{p,c})/2$  were in range of 0.32–0.43 V, which is expected for ferrocene derivatives containing amide group connected with cyclopentadienyl ring [26]. The width of the peaks at half-maximum,  $\Delta E_{fwhm}$ , were always larger than theoretical value. In an ideal case, full-width at half-height of the peak is given by  $3.53RT/nF$  (90.6 mV at 25°C) [27]. The differences between experimental and theoretical values reflect the interactions (mainly repulsive) between redox

centers and also indicate that some fractions of redox sites can be located in different molecular environment than others, which leads to multiple formal potentials and broadening of the peak. The latter is probably the reason of wider peaks in case of SAM 3 and 4. These systems are formed by relatively short molecules, therefore, higher degree of disorder can be expected.

The cyclic voltammetry responses of all systems were stable and we did not observe any decrease in the charge during repetitive potential scans. Using charge associated with the oxidation of ferrocene sites, we calculated the surface coverage for adsorbed compounds (1)–(4). Assuming the close-packed layer of 6.6 Å diameter spheres (corresponding to ferrocene groups) the theoretical value of maximum coverage is about  $4.5 \times 10^{-10}$  mol/cm<sup>2</sup> (area per molecule 37 Å<sup>2</sup>) [28]. The values obtained in this work were close to the maximum theoretical coverage of ferrocene thiols adsorbed on gold, therefore, we conclude that SAMs 1–4 are densely-packed. However, the surface coverage decreases in order SAM 1 > SAM 2 > SAM 3 > SAM 4, which reflects the dependence of order and packing density of the electroactive monolayers on the length of the molecules forming the system [23,29,30].

The values of double layer capacitance for long-chain SAMs 1 and 2 were in the range 4–6 µF/cm<sup>2</sup>, while for the short-chain SAMs 3 and 4 in the range of 10–12 µF/cm<sup>2</sup>. These values reflect the order within the monolayer and its permeability towards electrolyte ions. The values of the double-layer capacitance for electrodes modified with SAMs 1, 2 and 5 are significantly lower than those measured for SAMs 3 and 4, but it is understood if we consider looser molecular packing density for SAMs 3 and 4. Moreover, SAMs 3 and 4 were formed by short molecules, which means that dielectric layer is relatively thin comparing to SAMs 1 and 2.

**Electron transfer efficiency for SAMs 1–4 on gold substrates.** On the basis of electrochemical results obtained for SAMs 1–4 it can be concluded that electron transfer rates for short-chain SAMs 3–4 are significantly higher than for SAMs 1 and 2, thus these monolayers may be useful as electronically conducting linkers to the Au support. The rate constants were determined from cyclic voltammograms using Laviron treatment [31]. The transfer coefficients were obtained from the slopes of the plot of peak potential vs.  $\ln v$ . The standard rate constants were calculated using equation [31]:

$$\ln k = \alpha \ln(1 - \alpha) + (1 - \alpha) \ln \alpha - \ln \left( \frac{RT}{nFv} \right) - \alpha(1 - \alpha) \frac{nF\Delta E_p}{RT} \quad (1)$$

where  $k$  is the standard rate constant,  $\alpha$  and  $(1 - \alpha)$  are cathodic and anodic transfer coefficients respectively,  $v$  is a scan rate,  $\Delta E_p$  is the difference between anodic and cathodic peak potentials, the other symbols have their usual meaning. The standard rate constants for SAM 1 and 2 were about 100 s<sup>-1</sup> and 200 s<sup>-1</sup> respectively. The rate of electron transfer through SAMs 3 and 4 was too fast to be measured using our experimental setup, which means that the values of the rate constants for these systems are at least 10<sup>4</sup> s<sup>-1</sup>. Very fast electron transfer observed for SAM 4 may be



also connected with the presence of aromatic unit in the chain, transferring efficiently electrons between the redox site and the electrode surface.

**Potentiometric behavior of gold electrodes modified with SAMs.** Two monolayers: SAM 4 exhibiting very fast electron transfer and the nonelectroactive SAM 5 without units that could increase the efficiency of electron transfer, were chosen for preliminary studies of potentiometric responses of the BSC gold electrodes modified with SAMs. The dynamic responses of these two types of sensors to changes in the  $\text{Fe}(\text{CN})_6^{3-}$  to  $\text{Fe}(\text{CN})_6^{4-}$  ratio are illustrated in Fig. 5. Sensors with SAM 4 showed faster potentiometric response, similar to that presented earlier for structures with bare gold surface (Fig. 3). When SAM 5 was employed, the response was slower.

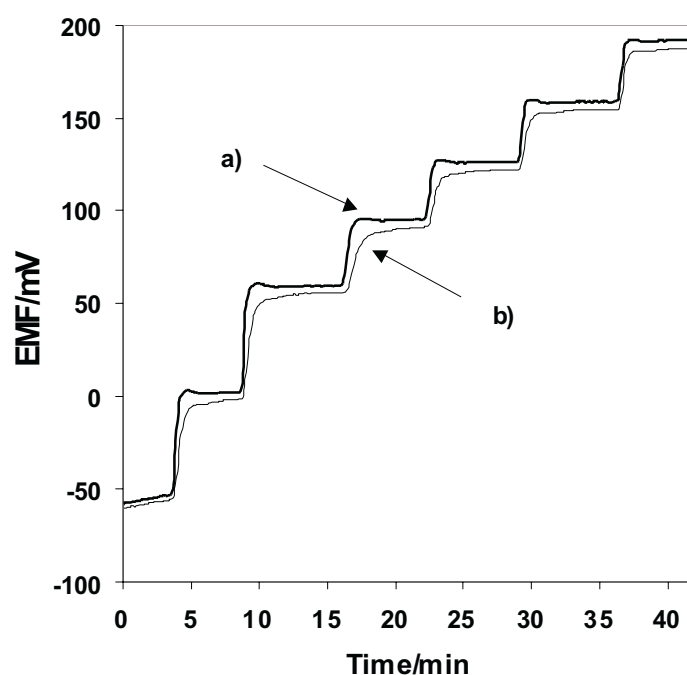


**Figure 5.** Potentiometric response to changes in  $\text{Fe}(\text{CN})_6^{3-}$  and  $\text{Fe}(\text{CN})_6^{4-}$  concentrations in sample solution for sensor chips with gold contact with monolayers: a) SAM 4 and b) SAM 5.

## CONCLUSIONS

BSC chips with Au contact either unmodified or modified with monolayers of purposely synthesized organothiol molecules gave stable electrode performances and short potentiometric response times for the  $[\text{Fe}(\text{CN})_6^{3-}/\text{Fe}(\text{CN})_6^{4-}]$  system in the solution. Voltammetric studies of the monolayers indicated electrochemically reversible behavior of the compounds and efficient coverage of the gold electrode.

Properties of 5 compounds were compared. The electrode modified with bis [4-((ferrocenylcarbonyl)amino)phenyl]disulfide (SAM 4) showed faster potentiometric response than covered with nonelectroactive alkanethiol monolayer, close to the response of bare gold. Thus, it provides efficient electronic wiring to the electrode and at the same time forms a hydrophobic barrier between the electrode and the solution eliminating direct access of solution species to the gold surface. These properties are important for the application of bis [4-((ferrocenylcarbonyl)amino)phenyl]disulfide as the component of intermediate layers in membrane ion-selective electrodes and work in this direction is continued in our laboratories.

#### Acknowledgments

The authors gratefully acknowledge the Polish State Committee for Scientific Research (4T10C 018 24) for financial support of this work.

#### REFERENCES

1. Cattrall R.W., Drew D.W. and Hamilton I.C., *Anal. Chim. Acta*, **76**, 269 (1976).
2. Janata J., Principles of Chemical Sensors, Plenum Press, New York, 1989.
3. Hauser P.C., Chiang D.W.L. and Wright G.A., *Anal. Chim. Acta*, **302**, 241 (1995).
4. Liu D., Meruva R.K., Brown R.B. and Meyerhoff M.E., *Anal. Chim. Acta*, **321**, 173 (1996).
5. Oyama N., Ohsaka T., Yoshimura F., Mizunuma M., Yamaguchi S., Ushizawa N. and Shimomura T., *J. Macromol. Sci. Chem.*, **A**, **25**, 1463 (1988).
6. Cadogan A., Gao Z., Lewenstam A., Ivaska A. and Diamond D., *Anal. Chem.*, **64**, 2496 (1992).
7. Bobacka J., McCarrick M., Lewenstam A. and Ivaska A., *Analyst*, **119**, 1985 (1994).
8. Pandey P.C. and Prakash R., *Sens. Actuators B*, **46**, 61 (1998).
9. Bobacka J., *Anal. Chem.*, **71**, 2932 (1999).
10. Zielińska R., Mulik E., Michalska A., Achmatowicz S. and Maj-Żurawska M., *Anal. Chim. Acta*, **451**, 173 (2001).
11. Vazquez M., Danielsson P., Bobacka J., Lewenstam A. and Ivaska A., *Sensors & Actuators B*, **97**, 182 (2003).
12. Fibbioli M., Bandyopadhyay K., Liu S-G., Echegoyen L., Enger O., Diederich F., Bühlmann P. and Pretsch E., *Chem. Comm.*, 339 (2000).
13. Fibbioli M., Bandyopadhyay K., Liu S-G., Echegoyen L., Enger O., Diederich F., Gingery D., Bühlmann P., Persson H., Suter U.W. and Pretsch E., *Chem. Mater.*, **14**, 1721 (2002).
14. Sęk S., Misicka A. and Bilewicz R., *J. Phys. Chem. B*, **104**, 5399 (2000).
15. Sęk S. and Bilewicz R., *J. Electroanal. Chem.*, **509**, 11 (2001).
16. Sęk S., Pałys B. and Bilewicz R., *J. Phys. Chem. B*, **106**, 5907 (2002).
17. Sęk S., Moszynski R., Sepiol A., Misicka A. and Bilewicz R., *J. Electroanal. Chem.*, **550**, 359 (2003).
18. Pijanowska D.G., Wyglądacz K., Jaźwiński J., Łysko J.M., Koszur J., Brzózka Z. and Malinowska E., *Proc. SPIE*, **4516**, 32 (2000).
19. Wyglądacz K., Malinowska E., Jaźwiński J. and Brzózka Z., *Sensors & Actuators B*, **83**, 109 (2002).
20. Chudy M., Dybko A., Wróblewski W. and Brzózka Z., *Anal. Chim. Acta*, **429**, 347 (2001).
21. Nuzzo R.G. and Allara D.L., *J. Am. Chem. Soc.*, **105**, 4481 (1983).
22. Li T.T. and Weaver M.J., *J. Am. Chem. Soc.*, **106**, 6107 (1984).
23. Porter M.D., Bright T.B., Allara D.L. and Chidsey C.E.D., *J. Am. Chem. Soc.*, **109**, 3559 (1987).
24. Brzózka Z., *Pomiary, Automatyka, Kontrola*, **9**, 179 (1988).
25. Wyglądacz K., Durnaś M., Parzuchowski P., Brzózka Z. and Malinowska E., *Sensors & Actuators B*, **95**, 366 (2003).

- 
26. Sabapathy R.C., Bhattacharyya S., Leavy M.C., Cleland W.E. and Hussey C.L., *Langmuir*, **14**, 124 (1998).
  27. Brown A.P. and Anson F.C., *Anal. Chem.*, **49**, 1589 (1977).
  28. Chidsey C.E.D., Bertozzi C.R., Putvinski T.M. and Mujcsce A.M., *J. Am. Chem. Soc.*, **112**, 4301 (1990).
  29. Bain C.D., Troughton E.B., Tao Y.-T., Evall J., Whitesides, G.M. and Nuzzo R.G., *J. Am. Chem. Soc.*, **111**, 321 (1989).
  30. Evans S.D. and Ulman A., *Chem. Phys. Lett.*, **170**, 462 (1990).
  31. Laviron E., *J. Electroanal. Chem.*, **52**, 395 (1974).